Polyphosphoinositides Inhibit the Interaction of Vinculin with Actin Filaments*

By: Paul A. Steimle, Jason D. Hoffert, Nils B. Adey, and Susan W. Craig

Steimle, P.A., Hoffert, J.D., Adey, N.B, Craig, S.W. (1999) Polyphosphoinositides inhibit the interaction of vinculin with actin filaments. *Journal of Biological Chemistry*. 274:18414-18420.

Abstract:

Binding of vinculin to adhesion plaque proteins is restricted by an intramolecular association of vinculin's head and tail regions. Results of previous work suggest that polyphosphoinositides disrupt this interaction and thereby promote binding of vinculin to both talin and actin. However, data presented here show that phosphatidylinositol 4,5-bisphosphate ($PI4,5P_2$) inhibits the interaction of purified tail domain with F-actin. Upon re-examining the effect of $PI4,5P_2$ on the actin and talin-binding activities of intact vinculin, we find that when the experimental design controls for the effect of magnesium on aggregation of $PI4,5P_2$ micelles, polyphosphoinositides promote interactions with the talin-binding domain, but block interactions of the actin-binding domain. In contrast, if vinculin is trapped in an open confirmation by a peptide specific for the talin-binding domain of vinculin, actin binding is allowed. These results demonstrate that activation of the actin-binding activity of vinculin requires steps other than or in addition to the binding of $PI4,5P_2$.

Article:

Vinculin, a 117-kDa component of microfilament-associated cell junctions (1), is a modular protein composed of a 95-kDa N-terminal, globular head domain connected by a short proline-rich region to a 30-kDa tail domain (reviewed in Ref. 2). Vinculin has an essential role in embryogenesis (3, 4) and regulatory roles in adhesion, spreading, and motility of cells in culture (5-10). Vinculin probably functions by interacting with particular structural and regulatory proteins found at focal contacts and *zonulae adherens* (11). Biochemical experiments with purified proteins show that the binding sites on vinculin for talin (12), F-actin (13), acidic phospholipids (14), and vasodilator-stimulated phosphoprotein (15), and sites for protein kinase C-mediated phosphorylation (16, 17), are blocked by the intramolecular association ($K_d \sim 50$ nM) of the head (V_h) and tail (V_t) regions (12). Therefore, regulation of the head-tail interaction to expose cryptic ligand binding and regulatory sites is hypothesized to be critical for recruitment of vinculin to sites of cell adhesion and/or for vinculin-dependent assembly of focal adhesion complexes (13). Elucidation of the factors that regulate the head-tail interaction is central to understanding how events at the cell surface are expressed ultimately in the activities of molecules directly responsible for the functions of focal adhesion plaques.

Evidence from *in vitro* experiments shows that acidic phospholipids in general (16), or specifically $PI4,5P_2$ [1] (18) block the interaction of purified head and tail domains and act on intact vinculin to expose the binding sites for talin on V_h (18) and for F-actin on V_t (16, 18). This observation provides a mechanistic link between cell surface receptors that modulate the synthesis of $PI4,5P_2$, a signaling molecule (19) and vinculin, a structural molecule involved in assembling a focal adhesion plaque and mediating anchorage to the actin cytoskeleton.

Here we provide new information that modifies the proposed role of $PI4,5P_2$ in activation of vinculin. In particular, we report that occupancy of the lipid-binding sites in purified tail domain prevents occupancy of the actin-binding sites. The effect of $PI4,5P_2$ on the interaction of purified V_t with F-actin had not been examined in previous studies. Therefore, to evaluate the apparent inconsistency of our result with the proposed role of

$PI4,5P_2$ on the actin binding activity of vinculin, we have used a novel peptide probe of vinculin conformation to re-assess the effects of acidic phospholipids, including polyphosphoinositides, on the actin- and talin-binding activities of vinculin. We find that when the experiments are controlled for the effect of $MgCl_2$ on the aggregation of $PI4,5P_2$ micelles, the results support a modified model in which the role of $PI4,5P_2$ is to expose the talin-binding site on vinculin while blocking the actin-binding site.

EXPERIMENTAL PROCEDURES

Protein Purification

Chicken smooth muscle vinculin and its 95-kDa head fragment were purified (14, 20, 21) and stored at 4 °C in TEEAN (10 mM Tris-HCl, pH 7.5, 1 mM EGTA, 0.1 mM EDTA, 150 mM and 3 mMNaN_3), 0.5% βME, 2 × protease inhibitor mixtures, PIC I and II. PIC I was added from a 1,000 × stock containing 1 mg/ml leupeptin, 2 mg/ml antipain, 10 mg/ml benzamidine, 10 KIU/ml aprotinin in H_2O. PIC II (1,000 ×) contains 1 mg/ml chymostatin, 1 mg/ml pepstatin in dimethysulfoxide. Vinculin was dialyzed against H_2O, 0.5% βME containing 2 × PIC I and II before its use in pVR binding experiments containing phospholipids. Rabbit skeletal muscle actin was purified as described previously (22) but with an additional gel exclusion chromatography step (23). Purified G-actin was stored in buffer A (2 mMTris-HCl, pH 7.5, 0.2 mM $CaCl_2$, 0.2 mM ATP, and 0.5 mM βME).

GST- and 6·His-tagged Fusion Proteins

GST/V884–1066 was constructed and purified as has been described (12) and stored at 4 °C in TEEAN. For experiments requiring untagged vinculin tail fragment, V884–1066 was expressed as a 6-histidine (His)-tagged fusion protein. Construction of 6-His/V884–1066 involved polymerase chain reaction amplification of the appropriate region of the chick embryo vinculin cDNA (24) using in-frame primers. The forward and reverse primers contained *Nde*I and *Xho*I sites, respectively. The amplified product was ligated into pCR2.1 vector (Invitrogen, San Diego, CA) according to the manufacturer's instructions, except that recombinants were transformed into competent*Escherichia coli* DH5α cells. Recombinant plasmid was digested with *Nde*I and *Xho*I to yield the insert fragment containing the polymerase chain reaction-amplified coding region and flanking vector sequence. The fragments were gel-purified using the Qiagen gel extraction kit (Chatsworth, CA) and ligated into the *Nde*I and *Xho*I sites of the pET-15b vector (Novagen, Madison, WI). As described in the manufacturer's instructions (pET System Manual; Novagen), 6·His/V884–1066 was expressed, purified, and then cleaved with thrombin to remove the 6·His tag. V884–1066 was dialyzed against TEEAN containing 0.5% βME and 2 × PIC I and II and quantified spectrophotometrically (E_{m}^{280} = 18,350) at 280 nm.

Peptide Synthesis

The pVR peptide (KKKSTGGFDDVYDLARRVSSALTTTLVATRPK) with and without biotin added to the N terminus was synthesized using an Applied Biosystems 430 peptide synthesizer, purified by high pressure liquid chromatography, and sequenced by automated Edman degradation at the Biosynthesis and Sequencing Facility, Johns Hopkins University School of Medicine (Dept. Biological Chemistry), Baltimore, MD. Biotinylated pVR was characterized by mass spectrometry at the JHU School of Medicine (Dept. Pharmacology) Mass Spectrometry Center, Baltimore, MD.

Phospholipid Vesicles

Phosphatidylcholine, PI, and phosphatidylserine were purchased as chloroform stocks from Avanti Polar Lipids (Alabaster, AL) and stored at −20 °C. PI4P and $PI4,5P_2$ were obtained as lyophilized powders from Sigma and were resuspended in distilled H_2O, 0.5% βME, and stored (4 °C) for use in assays. PI3P, $PI3,4P_2$, and $PI3,4,5P_3$ were purchased from Matreya, Inc. (Pleasant Gap, PA) as vacuum-dried powders and then resuspended in chloroform for storage at −20 °C.

For the preparation of phosphatidylcholine, PI, and phosphatidylserine small unilamellar vesicles, chloroform stocks of these phospholipids were dried under N_2 and then swollen at 5 mg/ml in distilled H_2O, 0.5% βME,

and then sonicated (30 min, 25 °C) in a Branson bath sonicator at the highest power setting. Small unilamellar vesicles containing both PI and PI4,5P_2at the desired ratios were prepared by adding the required amount of PI4,5P_2 (in distilled H_2O, 0.5% βME) to a known amount of dried PI and then sonicating as described. PI3P, PI3,4P_2, and PI3,4,5P_3 were dried under N_2 and resuspended in H_2O, 0.5% βME before sonication (30 min, 25 °C). Likewise, solutions of PI4P and PI4,5P_2 were sonicated (30 min, 25 °C) before use in assays. Phospholipid concentrations were determined by inorganic phosphate analysis using the Ames method (25).

Actin Polymerization

Unless indicated otherwise, actin polymerization was induced by the addition of 100 mM KCl and 2 mM $MgCl_2$ from a concentrated stock solution as described previously (13). For F-actin binding assays containing lipid, the $MgCl_2$ concentration was reduced to 2 μM to eliminate background sedimentation of vinculin and vinculin tail fragment. For experiments in low magnesium, actin polymerization was initiated by adding 100 mM KCl and 0.1 μM sonicated (30 s, 25 °C) F-actin seed (polymerized 2 h, 25 °C by the addition of 100 mM KCl and 0.1 mM $MgCl_2$ to a solution of 5 μMG-actin containing buffer A, 0.2 mM ATP, and 1 mM EGTA) to the reaction mix (26).

Precomplexing of pVR to Streptavidin-Alkaline Phosphatase

To complex pVR with streptavidin-conjugated alkaline phosphatase (SaAP), 4 μM biotinylated-pVR was incubated (1 h, 25 °C) with 20 units/ml SaAP (Boehringer-Mannheim) in a 100-μl reaction mix. After incubation, 5 μl of saturated (0.22 mg/ml) biotin was added to the reaction mix and then incubated (0.5 h, 25 °C) to block the remaining biotin-binding sites of SaAP. The pVR·SaAP complex was diluted 1/40 for use on Western blots.

Western Blotting and Detection of Biotinylated pVR

Samples were resolved by SDS-PAGE (10%), transferred to nitrocellulose (Schleicher & Schuell) (27), and blocked with 10% BLOTTO in Tris-buffered saline (TBST; 10 mM Tris-HCl, pH 8.0, 150 mM NaCl, and 0.05% Tween 20). Blots containing immobilized vinculin and vinculin head fragment were probed (1 h, 25 °C) with SaAP·pVR complexes, washed (4 × 10 min, 25 °C) with TBST, and then treated with Nitroblue tetrazolium chloride and 5-bromo-4-chloro-3-indoyl phosphate (Sigma) in 0.1 mMTris-HCl (pH 9.5), 0.1 M NaCl, and 5 mM$MgCl_2$ for colorimetric detection of SaAP·pVR complexes bound to either immobilized vinculin or V_h. Methods specific to individual experiments are described in the figure legends.

Isolation and Analysis of Complexes with Biotinylated pVR

Complexes with biotinylated pVR were isolated by incubating (0.5 h, 25 °C, with inversion) assay mixtures with steptavidin(Sa)-agarose beads (Novagen) followed by low speed (2,000 rpm × 4 min) centrifugation. Equal volumes of the pellet and supernatant fractions were subjected to SDS-PAGE (10% polyacrylamide gel) analysis (28) and the amount of target protein bound to Sa-agarose·pVR complexes was determined by Coomassie Blue staining of the gels. For relative quantitation, stained gels were dried, scanned, and analyzed densitometrically with the NIH Image program.

RESULTS

Effect of Polyphosphoinositides and Other Acidic Phospholipids on Binding of V_t to Actin Filaments

PI4,5P_2presented in micellar form, blocks the interaction of purified vinculin tail (V884–1066) with F-actin (Fig.1 *A*, *lanes 1–8*). Although the standard buffer for actin polymerization includes 2 mM $MgCl_2$, experiments with micelles of pure PI4,5P_2 were done in 0.002 mM Mg^{2+}because 2 mM Mg^{2+} causes mixtures ofV_t and PI4,5P_2 to sediment in the absence of actin (Fig. 1 *A*, *lanes 9–12*). Reduction of the $MgCl_2$ concentration from 2 mMto 2 μM eliminated this problem (compare Fig.1 *A*, *lanes 11–14* and *lanes 3*,*4*, *7*, and *8*).

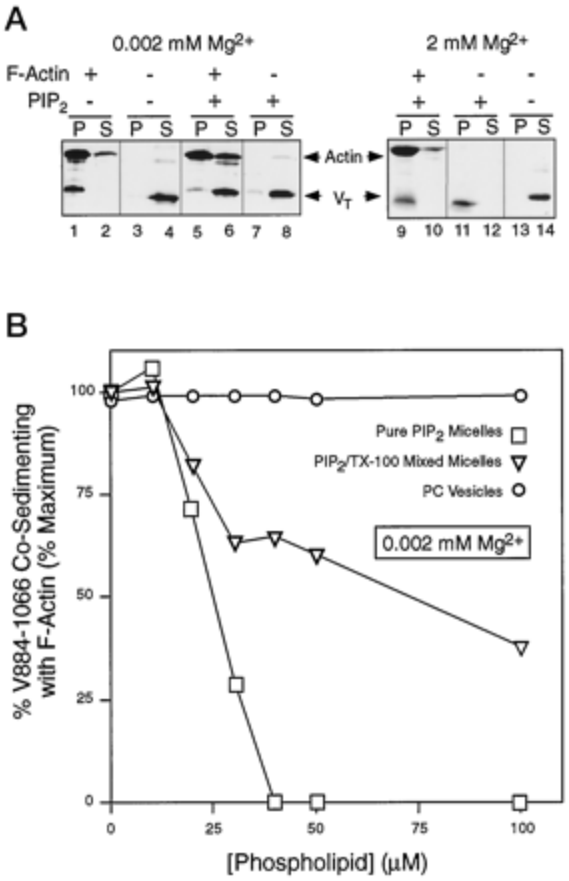

Figure 1

Effect of pure PI4,5P$_2$micelles and PI4,5P$_2$/Triton mixed micelles on the interaction of V$_t$ with F-actin. *A,* in a 100-μl reaction mix containing 3.2 mm Tris-HCl pH 7.1, 0.2 mm ATP, 100 mm KCl, 0.2 mm$CaCl_2$, 30 mm NaCl, 0.2 mm EGTA, 0.02 mm EDTA, and 0.5 mm βME; purified V884–1066 (V_t, 2 μm) was incubated (2 h at 25 °C) with 5 μm F-actin in the presence or absence of 100 μm pure PI4,5P_2 micelles (as indicated above each lane) and at either 2 mm or 2 μm $MgCl_2$ (as noted above each gel). After incubation, the reaction mixes (100 μl) were sedimented at 95,000 × *g* in a Beckman Airfuge and equal volumes of pellet (*P*) and supernatant (*S*) fractions were resolved by SDS-PAGE. In the presence of pure PI4,5P_2micelles there is a marked inhibition of V_t binding to F-actin (compare *lanes 1* and *2* with*lanes 5* and *6*). At 2 mm$MgCl_2$, V_t sediments to the same level in the absence of F-actin (*lanes 11* and *12*) as it does when F-actin is present (*lanes 9* and *10*) in the reaction mix; however, in the absence of both PI4,5$P_2$and F-actin, V_t remains in the supernatant (*lanes 13* and *14*). Reduction of the $MgCl_2$ concentration to 2 μm eliminates the background sedimentation of V_t (*lanes 7*and *8*). *B,* as described in *A*,V_t was assayed for F-actin binding activity at 2 μm $MgCl_2$ and over a range of lipid (pure PI4,5P_2 micelles, PI4,5P_2/Triton mixed micelles, or phosphatidylcholine/small unilamellar vesicle) concentrations. The relative amounts of V_t in the pellet and supernatant fractions were quantified by densitometric analysis of Coomassie Blue stained gels.

Presentation of PI4,5P_2 in the form of mixed micelles with Triton X-100 also inhibited interaction of V_t with F-actin (Fig. 1 *B*). Inhibition of the interaction ofV_t with actin by PI4,5P_2 presented either in micellar form or as mixed micelles with Triton X-100, is dependent on the concentration of lipid (Fig. 1 *B*). Phosphatidylcholine at up to 100 μM has no effect on F-actin binding by vinculin tail (Fig. 1 *B*). Analysis of other phospholipids revealed that PI4,5P_2/Triton X-100 mixed micelles (>200 μM), PI3,4P_2 (30 μM), PI3,4,5P_3 (30 μM), and phosphatidylserine (400 μM) inhibited completely the binding of purified vinculin tail to F-actin (data not shown).

Effect of PI4,5P$_2$ on the Actin-binding Activity of Vinculin

Because inhibition of the binding ofV_t to actin by PI4,5P_2 is not obviously consistent with a role of PI4,5P_2 in exposing a functional actin-binding site on vinculin, we wanted to confirm the effects of acidic phospholipids on the conformational state of vinculin by assaying for co-sedimentation of vinculin with F-actin in the presence of either PI4,5P_2/Triton X-100 mixed micelles (18) or pure PI4,5P_2 micelles (16). When the assay was controlled for the effect of $MgCl_2$ on the aggregation and sedimentation of PI4,5P_2 micelles, there was no co-sedimentation of vinculin with F-actin in the presence of micelles composed of pure PI4,5P_2 (Fig. 2, *A versus*

B). Divalent cations induce aggregation of $PI4,5P_2$ micelles (29), thus proteins bound to $PI4,5P_2$ micelles co-sediment with cation-induced $PI4,5P_2$ aggregates. Although the Mg^{2+}concentration does not affect the sedimentation of mixed micelles of $PI4,5P_2$ and Triton X-100, when these mixed micelles were examined at more than one concentration, they also failed to induce dose-dependent co-sedimentation of vinculin with F-actin even when the $PI4,5P_2$ concentration was raised to 100 μM (Fig. 2 *C*).

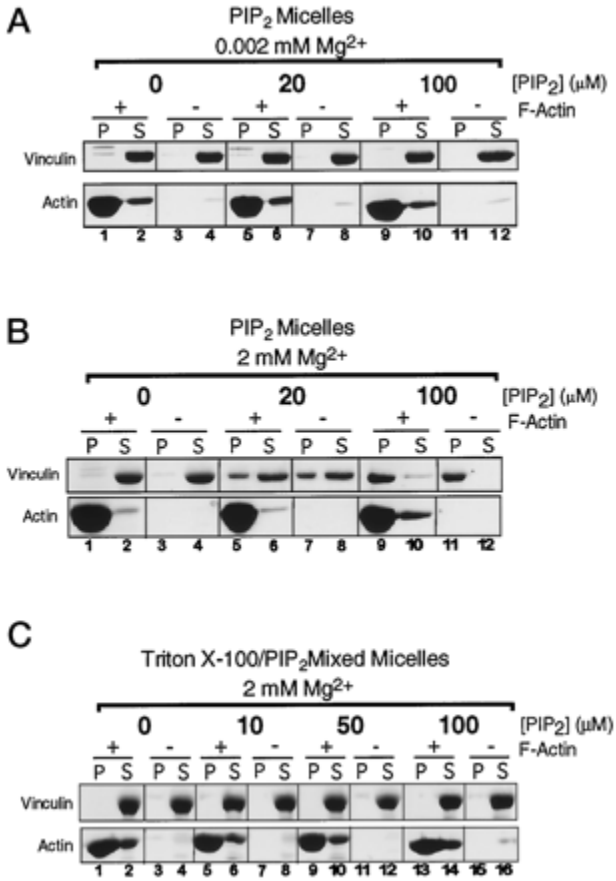

Figure 2

A, effect of pure $PI4,5P_2$micelles on the interaction of full-length vinculin with F-actin. As described in Fig. 1 *A*, purified vinculin (1 μm) was incubated (2 h, 25 °C, and 2 μm $MgCl_2$) with 5 μm F-actin in the presence or absence of either 20 μm or 100 μm $PI4,5P_2$ micelles as indicated above each lane. After incubation, the reaction mixes (100 μl) were sedimented at 95,000 × *g* in a Beckman Airfuge and equal volumes of pellet (*P*) and supernatant (*S*) fractions were resolved by SDS-PAGE. Comparison of*lanes 1–4* with *5–12* shows that in the presence of either 20 μm or 100 μm pure $PI4,5P_2$ micelles there is no detectable induction of vinculin binding to F-actin. *B*, effect of 2 mm$MgCl_2$ on the sedimentation of vinculin in the presence of pure $PI4,5P_2$ micelles. As has been described, 1 μm vinculin was assayed for F-actin binding activity at 2 mm $MgCl_2$ and in the presence or absence of either 20 μm or 100 μm pure $PI4,5P_2$ micelles as indicated above each lane. Under these conditions, sedimentation of vinculin is as high in the absence of F-actin (*lanes 3, 4, 7, 8, 11,* and *12*) as it is in the presence of F-actin (*lanes 1, 2, 5, 6, 9,* and*10*). Reduction of the $MgCl_2$ concentration to 2 μm eliminates this high background sedimentation of vinculin (compare with Fig. 2 *A*). In the absence of both $PI4,5P_2$ and F-actin, vinculin does not sediment when the $MgCl_2$ concentration is 2 mm (Fig.2 *B, lanes 3* and *4*). *C*,effect of $PI4,5P_2$/Triton mixed micelles on the interaction of vinculin with F-actin. Native vinculin was assayed as described in *A* for F-actin binding activity in the presence of 0, 10, 50, and 100 μm $PI4,5P_2$/Triton X-100 mixed micelles, as indicated above each lane, at 2 mm$MgCl_2$. $PI4,5P_2$/Triton X-100 mixed micelles do not induce vinculin co-sedimentation with F-actin. Note that there is no background sedimentation of vinculin at 2 mm$MgCl_2$ in the presence of $PI4,5P_2$/Triton X-100 mixed micelles (*lanes 7, 8, 11, 12, 15,* and*16*).

Characterization of Peptide pVR as a Probe of the Open Conformation of Vinculin

As an independent means of assessing the effect of acidic phospholipids on exposure of the actin- and talin-binding sites of vinculin, we have used a peptide (KKKSTGGFDDVYDLARRVSSALTTTLVATRPK) isolated from a phage-displayed random peptide library based on binding of phage to immobilized vinculin (30). This peptide, called pVR, inhibits binding of talin, but not α-actinin or paxillin, to immobilized vinculin, suggesting that the peptide binds at or near the talin-binding domain of vinculin. Control peptides bearing the same net positive charge as pVR but having distinct amino acid sequences do not bind to vinculin (30). Previous work

(30) demonstrated that although pVR binds to vinculin that has been adsorbed to polystyrene, polyvinylidene difluoride, or nitrocellulose (Fig.3 *B*), it does not bind to vinculin in solution (Fig. 3 *A*). The pVR binding site, located in the first 258 amino acid residues of the N-terminal head domain of vinculin, is made accessible for solution-based assays by removing the C-terminal tail domain of vinculin, residues 857–1066 (Fig. 3 *A*) (30), suggesting that the intramolecular head-tail interaction of vinculin blocks the binding site for pVR. That pVR is a specific probe for the open conformation of native vinculin is further supported by the finding that addition of purified vinculin tail domain to the reaction mix inhibits binding of pVR to vinculin head fragment in a dose-dependent fashion ($K_i \sim 0.4$ μM) (Fig. 4 *A*). This experiment shows that pVR binding occurs specifically to a site on V_h that is masked by V_t in the closed conformation of vinculin rather than to a new site created by unfolding of V_h after proteolytic removal of V_t. Conversely, pVR is able to compete binding of V_t to V_h with $\sim K_i = 0.3$ μM (Fig. 4 *B*) indicating that V_t and pVR interact at or near the same site on V_h. Collectively, these observations validate the use of pVR as a probe to identify the open conformation of full-length vinculin *in vitro*.

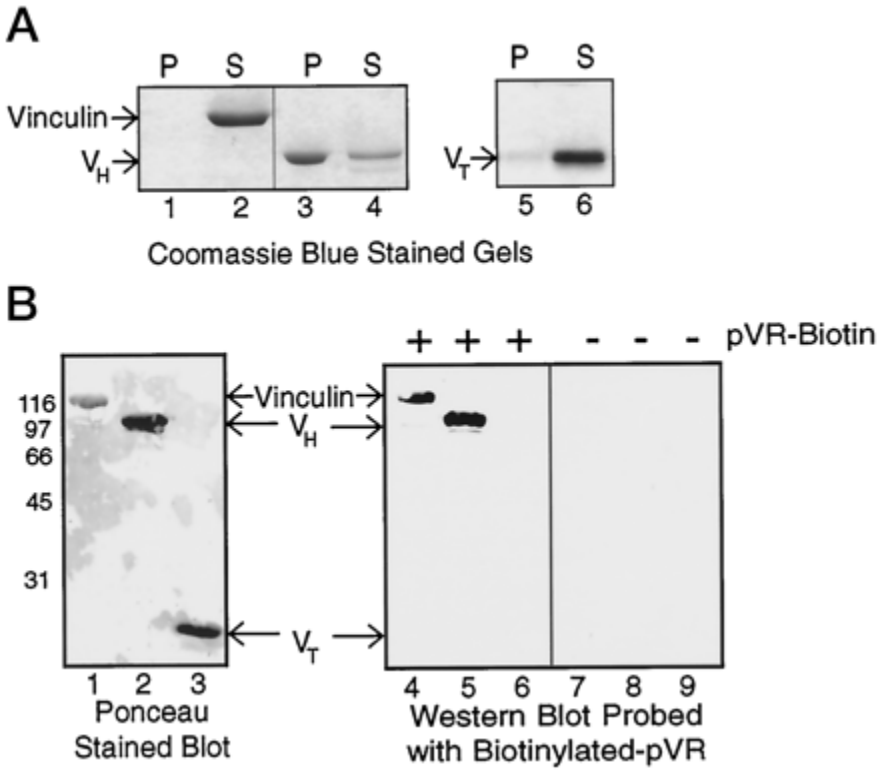

Figure 3

A, binding of pVR to full-length vinculin, 95-kDa vinculin head, and vinculin tail (V884–1066) in solution. Vinculin (0.5 μm), 95-kDa proteolytic head fragment (V_h, 0.5 μm), or vinculin tail fragment (V_t, 2 μm) was incubated (1 h, 25 °C, 50 μl reaction) with 5 μmbiotinylated-pVR in PBS and 0.01% BSA. Complexes with biotinylated pVR were isolated as described under "Experimental Procedures," and the amount of vinculin (*lanes 1* and *2*), V_h (*lanes 3* and *4*), and V_t (*lanes 5* and *6*) co-sedimenting with Sa-agarose·pVR complexes was assessed also as described. In the absence of pVR, there was no sedimentation of vinculin, V_h, or V_t with Sa-agarose beads (not shown). *B*, analysis of pVR binding to immobilized vinculin, V_h, and V_t. Purified vinculin (4.5 μg; *lanes 1*, *4*, and *7*), V_h (3 μg; *lanes 2*, *5*, and *8*), and V_t (5 μg; *lanes 3*, *6*, and *9*) were resolved by SDS-PAGE (10%), transferred to nitrocellulose and blocked as described under "Experimental Procedures." *Lanes 4–6* were incubated (1 h, 25 °C) with 0.1 μm biotinylated pVR precomplexed with SaAP and then developed as described under "Experimental Procedures." Binding of SaAP-bound pVR to immobilized vinculin and V_h was blocked by pre-incubation (1 h, 25 °C) with 10 μm nonbiotinylated pVR (not shown), and SaAP alone does not bind to immobilized vinculin, V_h, or V_t (*lanes 7–9*).

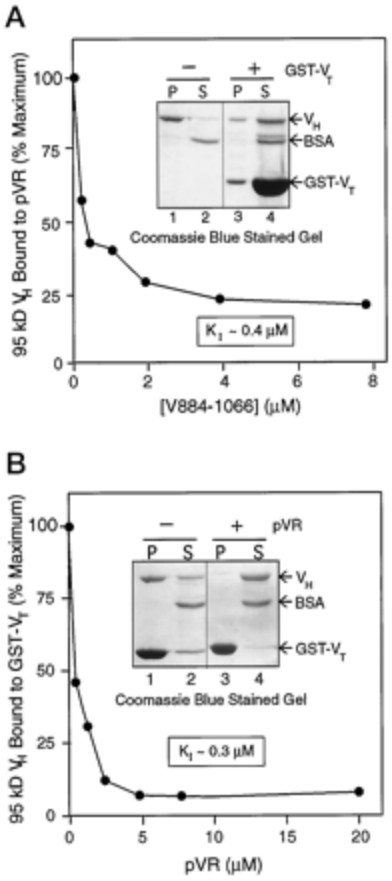

Figure 4

A, evaluation of pVR as a specific probe for the open conformation of vinculin *in vitro*.V_h (0.3 μm) was incubated (1 h, 25 °C, 50-μl reaction) with a range (0.25–8 μm) of GST-V884–1066 (*GST-*V_t) concentrations in PBS and 0.01% BSA before adding 1 μm (final concentration) biotinylated pVR to the reaction mix. Complexes with pVR were isolated as described, and the relative amounts ofV_h co-sedimenting with Sa-agarose·pVR complexes in the presence (*lanes 3* and *4*, *inset*) or absence (*lanes 1* and *2*, *inset*) of GST-V_t were quantified by densitometry of Coomassie Blue stained gels. The amount of V_h pelleting in the absence of GST-V_t represents 100% bound.*B*, competition of pVR for V_t binding toV_h . V_h (0.35 μm) was incubated (1 h, 25 °C, 50 μl reaction) with a range (0.5–20 μm) of pVR (nonbiotinylated) concentrations in PBS and 0.01% BSA before adding 1 μmGST-V_t to the reaction mix. GST·V_t complexes were isolated by incubating (0.5 h, 25 °C, with inversion) the reaction mixes with glutathione-agarose beads (Sigma) followed by low speed (2,000 rpm × 4 min) centrifugation. Coomassie Blue stained gels of the resulting pellets (*P*) and supernatants (*S*) were analyzed by densitometry to determine the relative amounts of $V_h$co-sedimenting with glutathione-agarose beads in the presence (*lanes 3* and *4*, *inset*) or absence (*lanes 1* and *2*, *inset*) of pVR. The amount of V_h pelleting in the absence of pVR represents 100% bound.

Effect of Polyphosphoinositides on Exposure of the Binding Site for pVR

Using biotinylated pVR to examine the effects of PI4,5P_2 exposure of the talin- and actin-binding sites on vinculin, we found that in 100 mM KCl only micelles of pure PI4,5P_2 (Fig. 5 *A*,*lanes 1–8*) and bilayer vesicles containing at least 50% PI4,5P_2 (Fig. 6 *B*) induce a dose-dependent opening of vinculin to expose the pVR binding site. Mixed Triton micelles containing up to 100 μM PI4,5P_2 did not activate vinculin for pVR binding (Fig. 5 *B*, *lanes 9–12*). To control for the possibility that pVR associates with vinculin through the mutual affinity of vinculin and pVR for PI4,5P_2 micelles rather than through a PI4,5P_2-induced exposure of the pVR binding site on vinculin, we examined the interaction of pVR with vinculin tail in the presence of PI4,5P_2. Although vinculin tail contains the high affinity PI4,5P_2 binding site (14), pVR does not bind to purified vinculin tail in the presence of PI4,5P_2(Fig. 5 *C*, *lanes 13–16*). Thus, polyphosphoinositide-induced binding of pVR to vinculin is mediated by the specific interaction of the peptide with its binding site in vinculin head domain.

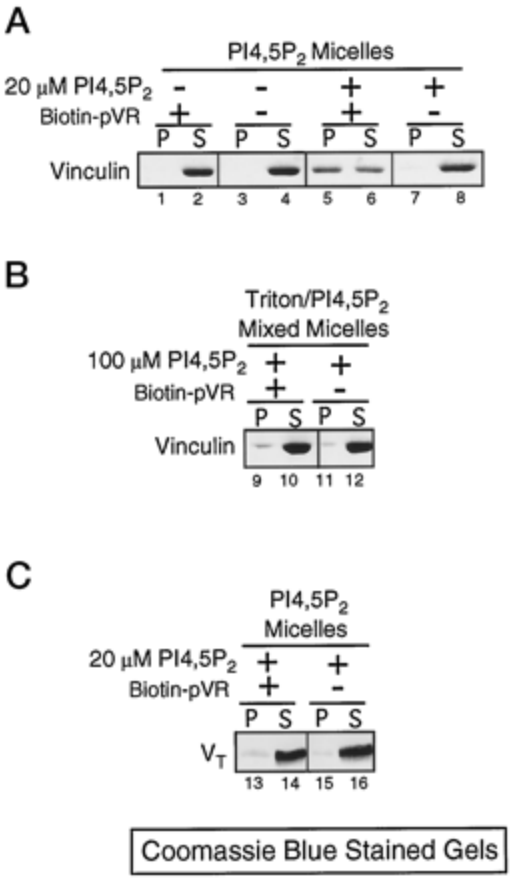

Figure 5

Effect of pure PI4,5P$_2$micelles and PI4,5P$_2$/Triton X-100 mixed micelles on the ability of vinculin to bind pVR in solution. *A,* reaction mix A (25 μl, 1.6 μm vinculin, 100 mm KCl, without lipid or with 40 μmPI4,5P$_2$) was incubated 0.5 h at 25 °C before adding reaction mix B (25 μl, 4 μm biotinylated pVR, 2× PBS, and 0.02% BSA) to give a 50-μl reaction volume containing 0.8 μm vinculin, 2 μm biotinylated pVR, 1× PBS, 0.01% BSA, and either no lipid or 20 μm pure PI4,5P$_2$ micelles. After incubating for 1 h at 25 °C, complexes with biotinylated pVR were isolated as described, and the amount of vinculin (*lanes 1–8*) co-sedimenting with Sa-agarose·pVR complexes was determined by SDS-PAGE of equal volumes of the supernatants (*S*) and pellets (*P*). In negative control reactions, nonbiotinylated pVR was used in place of biotinylated pVR as indicated by a (−) above the appropriate lanes. *B,* the pVR binding activity of native vinculin was assayed as described in *A* except that the final reaction mix contained 100 μm PI4,5P$_2$/Triton X-100 mixed micelles instead of pure PI4,5P$_2$ micelles (*lanes 9–12*). Under these conditions there is no induction of pVR binding by vinculin. *C,* as a control for PI4,5P$_2$bridging of pVR to the lipid binding region in vinculin tail, 2 μm V884–1066 (V_t) was used in place of vinculin in experiments containing PI4,5P$_2$ (*lanes 13–16*).

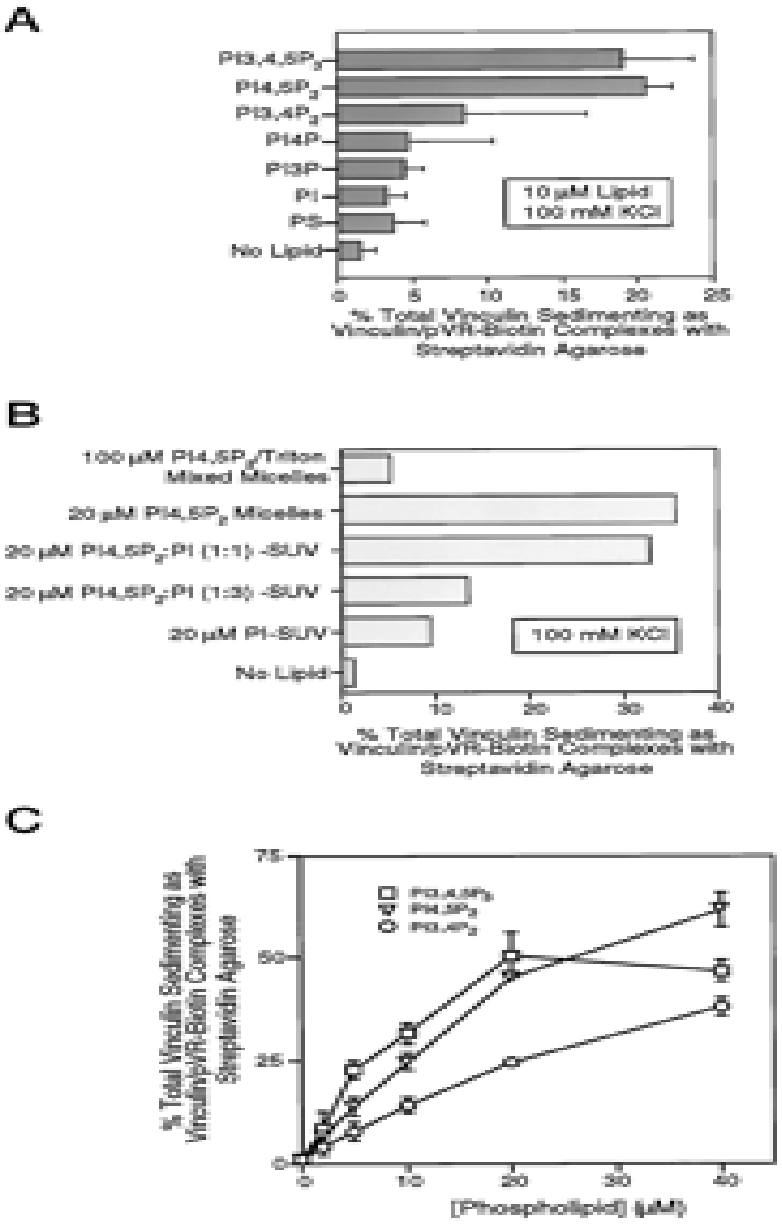

Figure 6

A, abilities of various acidic phospholipids to induce pVR binding by vinculin. Reaction mix A (see Fig. 5 *A*) with or without 10 μm lipid (phosphatidylserine, PI, PI3P, PI4P, PI3,4P_2, PI4,5P_2, or PI3,4,5P_3 as indicated) was incubated (0.5 h at 25 °C, 50-μl reaction). Reaction mix B (see Fig. 5 *A*) was then added, and the reaction was then incubated for 1 h at 25 °C. Complexes with biotinylated pVR were isolated and analyzed as described, and the relative amounts of vinculin co-sedimenting with Sa-agarose·pVR complexes were determined. Plotted values represent the mean of three independent determinations, and bars indicate the mean ± S.E. *B,* effects of phospholipid packing on activating vinculin to bind pVR. The pVR binding activity of native vinculin was assayed (as described for Fig.6 *A*) in the presence of either pure PI4,5P_2micelles, PI4,5P_2/Triton X-100 mixed micelles, or mixed vesicles of PI4,5P_2 and PI (at the ratios indicated in the figure). *C,* relative ability of different polyphosphoinositides to open vinculin for pVR binding. The level of pVR binding by vinculin was determined (as described for Fig.6 *A*) at physiologic ionic strength (100 mm KCl) in the presence of 0, 2, 5, 10, 20, and 40 μmPI3,4P_2, PI4,5P_2, or PI3,4,5P_3. Plotted values represent the mean of three independent determinations; error bars indicate the plotted mean ± S.E.

Among the acidic phospholipids tested, only the polyphosphoinositides (PI3,4P_2, PI4,5P_2, and PI3,4,5P_3) activated vinculin for pVR binding (Fig. 6 *A*) when the assay was performed in at least 100 mM salt. This polyphosphoinositide-induced activation of vinculin is dose-dependent (Fig. 6 *C*) and peaks at about 40 μM lipid. When the concentration of polyphosphoinositide is >40 μM, the level of pVR binding by vinculin decreases due to an apparent interaction between pVR and polyphosphoinositide at high concentrations of phospholipid (data not shown). Vinculin also binds to pVR when PI4,5P_2 is presented in mixed vesicles with PI. However, maximal activation occurs only when PI4,5P_2 represents at least 50% of the vesicular lipid (Fig. 6 *B*).

pVR Induces Actin-binding Activity in Vinculin

The preceding results indicated that pVR could be used to determine whether vinculin in the open conformation can bind F-actin when the actin-binding site is not occluded by $PI4,5P_2$. In solution, the closed conformation of vinculin is favored strongly because of the high affinity of the head-tail interaction and the fact that head and tail interact intramolecularly. However, equilibrium kinetics predicts that vinculin can be trapped kinetically in open form in the presence of a large molar excess of a ligand that inhibits the intramolecular head-tail interaction. pVR blocks the bimolecular interaction between the purified head and tail fragments of vinculin with a K_i of ~ 0.3 μM (Fig.4 *B*), consistent with the affinity (K_d ~ 0.1 μM) of pVR for vinculin head (30). When the concentration of pVR is raised to 6,000-fold molar excess over the K_d determined for the bimolecular interaction of head and tail (K_d ~ 50 nM), vinculin becomes competent to bind F-actin (Fig.7). This effect of pVR on binding of vinculin to actin is specific because 95-kDa head fragment alone does not co-sediment with F-actin at similar concentrations of pVR. Sedimentation of vinculin requires the presence of both pVR and F-actin, and sedimentation of vinculin with actin depends upon the amount of pVR present (Fig. 7).

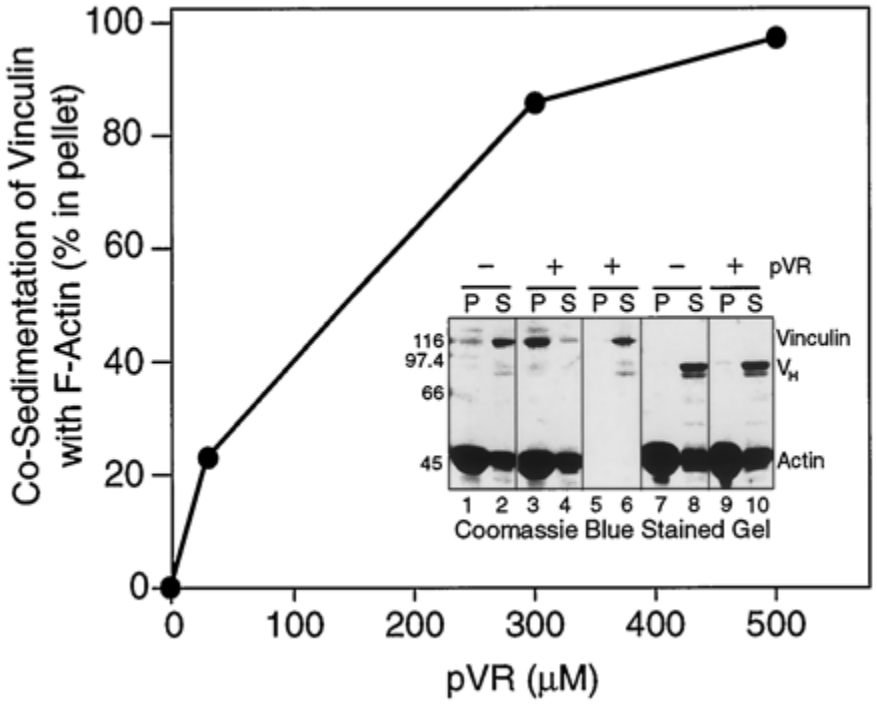

Effect of pVR, a competitive ligand for the head-tail interaction, on opening of vinculin for F-actin binding. Vinculin (0.44 μM) was incubated (1 h, 25 °C, 100-μl reaction) with 4.7 μM F-actin over a range (30–500 μM) of nonbiotinylated pVR concentrations in buffer A containing 2 mM $MgCl_2$ and 100 mMKCl before sedimentation at 95,000 × *g* in a Beckman Airfuge. Equal volumes of reaction pellets (*P*) and supernatants (*S*) were resolved by gel electrophoresis (as described) and Coomassie Blue stained gels were analyzed by densitometry to determine the relative amounts of vinculin that co-sediment with F-actin in the presence of pVR ligand (*lanes 3–6, inset*). Vinculin does not sediment when either pVR (*lanes 1* and *2*, *inset*) or F-actin (*lanes 5* and *6*, *inset*) is absent from the reaction mix and proteolytic head (V_h) does not co-sediment with F-actin in the presence of pVR (*lanes 9* and*10, inset*).

DISCUSSION

We have found that micellar PI4,5P2 enables vinculin to bind pVR, but does not allow binding to F-actin. This result is consistent with the observation that PI4,5P2 inhibits binding of F-actin to purified V t. We also show that vinculin does bind F-actin when the intramolecular interaction of head and tail is displaced by an ~6,000-fold molar excess of pVR over theK d for the bimolecular interaction of the purified head and tail domains. Previous studies have shown that PI4,5P2 and several other acidic phospholipids, inhibit the bimolecular interaction of purified head and purified tail (16, 18). In addition, there is partial overlap of vinculin's F-actin binding regions (residues 884–1012 and 1012–1066) (31, 32) and acidic phospholipid binding regions (residues 916–970 and 1012–1066) (33,34). Therefore, it is likely that PI4,5P2 inhibits the interaction of vinculin and V t with F-actin by occluding the actin-binding site. Altogether, the data are consistent with a model in which

polyphosphoinositides presented in the form of micelles displace the head domain of vinculin by binding to the tail domain. Ligand-binding sites in V h are unmasked, but the F-actin binding sites in V t are occluded by the bound phospholipid (Fig. 8). Based on earlier work (33), the tail domain of open vinculin will be partially buried in the hydrophobic core of the lipid micelles (Fig. 8).

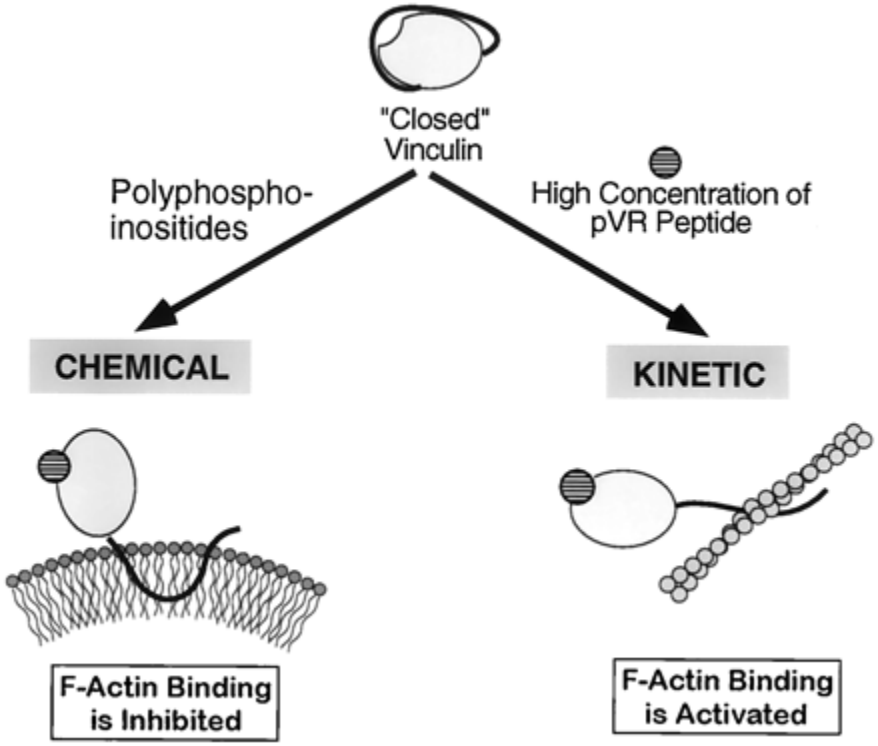

Figure 8
Cartoon illustrating the differential effect of pVR and polyphosphoinositides on exposure of the talin- and actin-binding sites in vinculin. PIP_2 binds to the tail domain of vinculin and disrupts the intramolecular interaction with the head domain. As a result, the talin-binding site inV_h becomes accessible, but the actin-binding sites in V_t are blocked by the bound PIP_2. pVR displaces the head-tail interaction by binding at or near the talin-binding site on V_h leavingV_t free to associate with F-actin.

Several other actin-binding proteins are also inhibited by $PI4,5P_2$ (35) and recent structural evidence suggests a common mechanism of $PI4,5P_2$ action. The atomic structure of gelsolin indicates that polyphosphoinositides compete with F-actin for binding to overlapping, solvent-exposed sites on plasma gelsolin (36). Evidence also suggests a competitive mechanism for $PI4,5P_2$disruption of profilin-actin (37) and destrin-actin (38) complexes. A possible source of the difference between our results on the effects of micellar $PI4,5P_2$ and those reported previously (16) is the concentration of $MgCl_2$ used in the buffer for actin-binding assays. We observed that when 2 mM$MgCl_2$ was a component of the actin polymerization buffer (as in Ref. 16), addition of pure $PI4,5P_2$ micelles to the assay mix caused sedimentation of vinculin and vinculin tail in the absence of F-actin. At millimolar concentrations of divalent cation, $PI4,5P_2$ micelles form large aggregates that pellet at speeds required to sediment F-actin (29). Under these conditions, proteins that bind to $PI4,5P_2$ also sediment. The published data does not exclude the possibility that the $MgCl_2$ effect on aggregation of $PI4,5P_2$ micelles is a source of the difference between our results and those of Weekes *et al.*(16).

Our data indicates that the physical packing of polyphosphoinositides in pure micelles is crucial for opening vinculin because mixed micelles of Triton X-100 and $PI4,5P_2$ are unable to cause binding of pVR or F-actin to vinculin. This finding is inconsistent with an earlier report that mixed micelles containing 0.33 molecules of $PI4,5P_2$/Triton micelle (10 μM$PI4,5P_2$) activates vinculin to bind both talin and F-actin (18). In our experiments, there is not a dose-dependent effect of mixed micelles containing from 0.33–3 molecules of $PI4,5P_2$ per micelle on co-sedimentation of actin and vinculin. Although it is possible that we have not reproduced exactly the conditions of the previous report, the absence of data demonstrating a dependence of vinculin co-sedimentation with F-actin on the amount of $PI4,5P_2$ in the Triton micelles (18), together with the

results presented here, argues against a role for PI4,5P_2 in exposing the actin-binding activity of vinculin. This conclusion is strengthened by the demonstration of dose-dependent inhibition of F-actin binding to purifiedV_t by PI4,5P_2 micelles and by PI4,5P_2/Triton mixed micelles.

Using pVR as a probe for the talin-binding conformation of vinculin, we examined the effects of various acidic phospholipids on exposure of the talin-binding site on vinculin. In buffers containing at least 100 mM KCl, only pure micelles of the polyphosphoinositides (PI3,4P_2, PI4,5P_2, and PI3,4,5P_3) induce a dose-dependent binding of pVR to vinculin. The finding that 3-phosphorylated inositol lipids can induce conformational change in vinculin suggests that intracellular signaling through phosphoinositide 3-kinase (to produce PI3,4P_2 and PI3,4,5P_3), along with those signals mediating PI4,5P_2 levels, may also be important in vinculin activation.

Evidently, differential exposure of various ligand-binding sites on vinculin can be achieved depending on the mechanism of conformational alteration. For example, PI4,5P_2-induced changes in vinculin unmask the talin and pVR-binding site but block the actin-binding sites, whereas pVR-induced changes occupy the talin-binding site and expose the actin-binding sites (Fig. 8). The implication is that depending on the mechanism of activation, vinculin might be assembled into complexes that differ by virtue of which ligand-binding sites on vinculin are functional. This provides a potential mechanism for building functionally dissimilar protein complexes from the same repertoire of protein components.

Currently it is thought that signal transduction events stimulate the local synthesis of PI4,5P_2 at focal adhesions. This newly synthesized PI4,5P_2 then recruits and/or opens vinculin to expose the sites for talin and F-actin, thereby contributing to assembly of plaque components and linkage of actin to the plasma membrane (18). However, our results indicate that in order for PI4,5P_2-bound vinculin to bind actin, the PI4,5P_2 would have to be hydrolyzed or displaced from vinculin. PI4,5P_2 hydrolysis could occur by the action of a specific phospholipase or phosphatase, making the induction of vinculin's actin-binding activity a two step process. Alternatively, vinculin might be activated by yet unknown mechanisms that expose both the talin- and actin-binding activities.

ACKNOWLEDGEMENTS

We thank Jodie Franklin and Jennifer Senft for synthesis, purification, and sequencing of pVR, and Amina S. Woods for the mass spectrometry of biotinylated pVR.

Footnotes

- * This work was supported by research Grant GM41605 from the National Institutes of Health and by a grant from the Muscular Dystrophy Association.The costs of publication of this article were defrayed in part by the payment of page charges. The article must therefore be hereby marked "*advertisement*" in accordance with 18 U.S.C. Section 1734 solely to indicate this fact.

ABBREVIATIONS

$PI4,5P_2$ phosphatidylinositol 4,5-bisphosphate

BSA bovine serum albumin

GST glutathione *S*-transferase

βME β-mercaptoethanol

PI phosphatidylinositol

PI3P phosphatidylinositol 3-phosphate

PI4P phosphatidylinositol 4-phosphate

$PI3,4P_2$ phosphatidylinositol 3,4-bisphosphate

$PI3,4,5P_3$ phosphatidylinositol 3,4,5-triphosphate

Sa streptavidin

SaAP SA-conjugated alkaline phosphatase

PAGE polyacrylamide gel electrophoresis

V_h head domain of vinculin

V_t tail domain of vinculin

PBS phosphate-buffered saline

REFERENCES

Geiger B., Tokuyasu K. T., Dutton A. H., Singer S. J.(1980) Proc. Natl. Acad. Sci. U. S. A. 77:4127–4131.

Winkler J., Lunsdorf H., Jockusch B. M.(1996) J. Struct. Biol. 116:270–277.

Barstead R. J., Waterston R. H.(1991) J. Cell Biol. 114:715–724.

Weiming X., Baribault H., Adamson E. D.(1998) Development 125:327–337.

Coll J.-L., Ben-Ze'ev A., Ezzell R. M., Rodriguez Fernandez J. L., Baribault H., Oshima R. G., Adamson E. D. (1995) Proc. Natl. Acad. Sci. U. S. A. 92:9161–9165.

Volberg T., Geiger B., Kam Z., Pankov R., Simcha I., Sabanay H., Coll J.-L., Adamson E., Ben-Ze'ev A.(1995) J. Cell Sci. 108:2253–2260.

Weiming X., Coll J.-L., Adamson E. D.(1998) J. Cell Sci. 111:1535–1544.

Rodriguez Fernandez J. L., Geiger B., Salomon D., Sabanay I., Zoller M., Ben-Ze'ev A.(1992) J. Cell Biol. 119:427–438.

Rodriguez Fernandez J. L., Geiger B., Salomon D., Ben-Ze'ev A.(1993) J. Cell Biol. 122:1285–1294.

Rodriguez Fernandez J. L., Geiger B., Salomon D., Ben-Ze'ev A.(1992) Cell Motil. Cytoskeleton 22:127–134.

Goldmann W. H., Ezzell R. M., Adamson E. D., Niggli V., Isenberg G.(1996) J. Muscle Res. Cell Motil. 17:1–5.

Johnson R. P., Craig S. W.(1994) J. Biol. Chem. 269:12611–12619.

Johnson R. P., Craig S. W.(1995) Nature 373:261–264.

Johnson R. P., Craig S. W.(1995) Biochem. Biophys. Res. Commun. 210:159–164.

Huttelmaier S., Mayboroda O., Harbeck B., Jarchau T., Jockusch B. M., Rudiger M.(1998) Curr. Biol. 8:479–488.

Weekes J., Barry S. T., Critchley D. R.(1996) Biochem. J. 314:827–832.

Schwienbacher C., Jockusch B. M., Rudiger M.(1996) FEBS Lett. 384:71–74.

Gilmore A. P., Burridge K.(1996) Nature 381:531–535.

McNamee H. M., Ingber D. E., Schwartz M. A.(1992) J. Cell Biol. 121:673–678.

Feramisco J. R., Burridge K.(1980) J. Biol. Chem. 255:1194–1199.

Groesch M. E., Otto J. J.(1990) Cell Motil. Cytoskeleton 15:41–50.

Spudich J., Watt S.(1971) J. Biol. Chem. 246:4866–4871.

MacLean-Fletcher S., Pollard T. D.(1980) Biochem. Biophys. Res. Commun. 96:18–27.

Coutu M. D., Craig S. W.(1988) Proc. Natl. Acad. Sci. U. S. A. 85:8535–8539.

Ames B. N.(1966) Methods Enzymol. 8:115–118.

Pollard T. D(1983) Anal. Biochem. 134:406–412.

Mumby S. M., Buss J. E.(1990) METHODS: A Companion to Methods in Enzymology 1:216–220.

Laemmli U. K.(1970) Nature 227:680–685.

Flanagan L. A., Cunningham C. C., Chen J., Prestwich G. D., Kosik K. S., Janmey P. A.(1998) Biophys. J. 73:1440–1447.

Adey N. B., Kay B. K.(1997) Biochem. J. 324:523–528.

Johnson R. P., Craig S. W.(1995) Mol. Biol. Cell 6:341, (abstr.).

Huttelmaier S., Bubeck P., Rudiger M., Jockusch B.(1997) Eur. J. Biochem. 247:1136–1142.

Johnson R. P., Niggli V., Durrer P., Craig S. W.(1998) Biochemistry 37:10211–10222.

Tempel M., Goldmann W. H., Isenberg G., Sackmann E.(1995) Biophys. J. 69:228–241.

Janmey P. A.(1994) Annu. Rev. Physiol. 56:169–191.

Burtnick L. D., Koepf E. K., Grimes J., Jones E. Y., Stuart D. I., McLaughlin P. J., Robinson R. C.(1997) Cell 90:661–670.

Pollard T. D., Almo S., Quirk S., Vinson V., Lattman E. E.(1994) Annu. Rev. Cell Biol. 10:207–249.

Hatanaka H., Ogura K., Moriyama K., Ichikawa I., Inagaki F.(1996) Cell 85:1047–1055.